

**ICSO 2016**

**International Conference on Space Optics**

Biarritz, France

18–21 October 2016

*Edited by Bruno Cugny, Nikos Karafolas and Zoran Sodnik*



***First aircraft test results of a compact, low cost hyperspectral imager for earth observation from space***

*B. T. G. de Goeij*

*G. C. J. Otter*

*J. M. O. van Wakeren*

*J. P. Veefkind*

*et al.*



icso proceedings



International Conference on Space Optics — ICSO 2016, edited by Bruno Cugny, Nikos Karafolas,  
Zoran Sodnik, Proc. of SPIE Vol. 10562, 105621N · © 2016 ESA and CNES  
CCC code: 0277-786X/17/\$18 · doi: 10.1117/12.2296068

Proc. of SPIE Vol. 10562 105621N-1

## FIRST AIRCRAFT TEST RESULTS OF A COMPACT, LOW COST HYPERSPECTRAL IMAGER FOR EARTH OBSERVATION FROM SPACE

B.T.G. de Goeij<sup>1</sup>, G.C.J. Otter<sup>1</sup>, J.M.O. van Wakeren<sup>1</sup>, J.P. Veefkind<sup>2,3</sup>, T. Vlemmix<sup>3</sup>, X. Ge<sup>3</sup>,  
P.F. Levelt<sup>2,3</sup>, B.P.F. Dirks<sup>1</sup>, P.M. Toet<sup>1</sup>, L.F. van der Wal<sup>1</sup>, R. Jansen<sup>1</sup>

<sup>1</sup> TNO, PO Box 155, 2600 AD Delft, The Netherlands, +31 888666470, bryan.degoeij@tno.nl.

<sup>2</sup> KNMI, PO Box 201, 3730 AE De Bilt, The Netherlands

<sup>3</sup> TU Delft, PO Box 5048, 2628 CN Delft, The Netherlands

### I. INTRODUCTION

In recent years TNO has investigated and developed different innovative opto-mechanical designs to realize advanced spectrometers for space applications in a more compact and cost-effective manner. This offers multiple advantages: a compact instrument can be flown on a much smaller platform or as add-on on a larger platform; a low-cost instrument opens up the possibility to fly multiple instruments in a satellite constellation, improving both global coverage and temporal sampling (e.g. multiple overpasses per day to study diurnal processes); in this way a constellation of low-cost instruments may provide added value to the larger scientific and operational satellite missions (e.g. the Copernicus Sentinel missions); a small, lightweight spectrometer can easily be mounted on a small aircraft or high-altitude UAV (offering high spatial resolution).

Moreover, a low-cost instrument may allow us to break through the 'cost spiral': lower cost will allow us to take more technical risk and thus be more innovative. This will lead to a much faster development cycle than customary for current Earth-observation instruments.

Finally, the TNO designs offer flexibility to tune the performance (spectral range, spectral resolution) of the spectrometer to a specific application (like air quality, climate, water quality, etc.). Thus, based on the same basic system design, these instruments offer a wide range of applications to a variety of clients, both inside and outside the scientific community using a quasi-recurrent instrument (reducing the development cost for each instrument).

In this paper the most mature design of a hyperspectral imaging spectrometer (named 'Spectrolite') is used to illustrate this innovative approach. For this purpose chapter II will introduce the Spectrolite concept, design philosophy and breadboard (BB). Chapter III will discuss how the Breadboard was transformed into an airborne instrument (for a test flight over Berlin as part of AROMAPEX [7]) in the time frame of only a month. The (reduced) Level 0-1B data processor and corresponding characterization measurements (performed in only 5 days) are presented in Chapter IV, followed by achieved NO<sub>2</sub> retrieval results from the airborne test flight over Berlin in chapter V. Finally chapter VI will provide a conclusion and present the next steps for Spectrolite.

### II. SPECTROLITE

Spectrolite (Fig. 1) is a hyperspectral imaging spectrometer concept based on the technological heritage from TROPOMI. The instrument is designed as a low cost modular system for multiple applications (air quality, land use or water quality) and consists of an all-reflective, off-axis optical design.

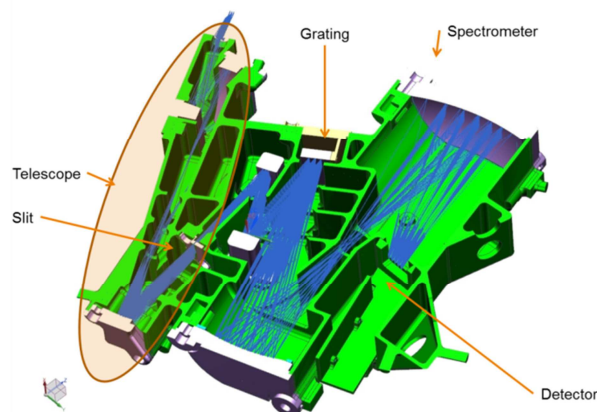


**Fig. 1.** 3D drawing of Spectrolite showing the housing (green), components (grey) and optical path (blue).

The all-reflective approach has a number of advantages:

- A favorable thermal stability due to the all-aluminum design.
- The design can be copied unchanged for other wavelength ranges between 270nm and 2400nm (with the exception of the grating and possibly the detector);
- Fewer optical elements due to the insensitivity to chromatic aberrations and the application of diamond turned free form optics;
- More design freedom regarding stray light baffling due to the off-axis nature of such a design;
- Inherently low ghost stray light between detector and optical surfaces.

Initial ideas about a Spectrolite type instrument started in a discussion between TNO, ESA and NSO [1]. After these initial discussions TNO continued to design and build a Spectrolite breadboard which has been in detail reported in [2] and of which the results are summarized in the next three sections.

#### *A. Spectrolite Design Philosophy*

In order to achieve the envisioned modularity and cost reduction the Spectrolite concept was designed according to a number of design principles in general and a specific optical design approach in particular.

The general design principles can be summarized as follows:

- Make a self-standing system that is optimized for a specific task (i.e. a single observable phenomenon); this keeps the development complexity relatively small and ensures that though requirements for different observable phenomena are not mingled, keeping the cost for development and production low.
- Make a modular system that can easily be adopted for different observable phenomena (e.g. air quality, land use or water quality) without a full redevelopment and qualification; this should allow the system to be built in small series, allowing the development cost to be shared over multiple modules.

Following these principles resulted in the overall concept in Fig. 1.

The chosen design optical approach was based on a semi-automated ('brute force') approach. The starting point was found using YYBAR diagrams and SEIDEL aberrations. From this starting point, 10 million design variations were explored by 'brute force' calculations. These 10 million variations were then filtered on parameters like volume, total track etc. Finally the designer chose the most promising/optimal solution for further processing. The optimum solution was the input for a CodeV model, which was allowed to optimize further using a number of geometrical constraints (for more details see [3]).

In the overall design approach free-form mirrors (TROPOMI technology) were introduced for greater optical design freedom. In traditional free-form systems, this advantage is typically used to boost the optical performance of the system. For Spectrolite it was used to increase the robustness of the design, creating a very stable instrument that can be quickly assembled on manufacturing tolerances. The nominal RMS spot size of the design is ~6.5 micron. Including quite large tolerances it is ~20 micron, which is sufficient for its intended purpose.

#### *B. Spectrolite Breadboard*

In order to demonstrate that the design philosophy worked, a Spectrolite breadboard was developed and built. The breadboard was optimized for the detection of NO<sub>2</sub> concentrations in the atmosphere. For this breadboard the following requirements were set:

- Spectral range of 320 nm – 500 nm
- Spectral resolution < 0.5 nm
- Spatial resolution of 0.1°
- Field of view of 60°
- Measurement SNR of 700 over urban areas

For the breadboard model only the spectrometer part was built without the (integrated) telescope. A separate external telescope and aperture was installed in front of the entrance slit. Commercial off-the-shelf (COTS) components were used. e.g. a non-optimized grating and detector. The etendu of the instrument was smaller than envisioned (partly due to the limited area of the detector which could be used). Nevertheless, it allowed to demonstrate the performance of this all-reflective spectrometer in aluminum housing.

The Spectrolite BB housing (See Fig.2) was manufactured using a relatively novel method for space hardware: 3D printing and investment casting. First, a 3D wax model was printed, from which a ceramic cast was made. The spatial accuracy of this process is in the order of 0.1 mm, which is insufficient if one wants to mount the mirrors directly without alignment. Therefore the mirror interfaces were post machined to an accuracy of 20 micron.

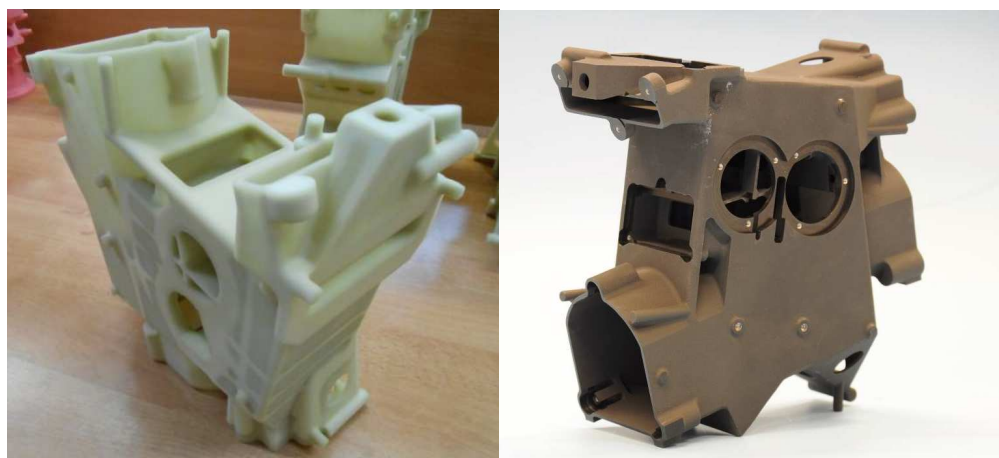


**Fig. 2.** The Spectrolite housing. On the left the wax model and on right the final (black anodized) structure.

The 4 mirrors of the spectrometer were manufactured at TNO using Single Point Diamond Turning with a slow servo tool. After this the mirrors were lightly hand polished only. The manufacturing turned out to be more challenging than e.g. the mirrors for Sentinel 5P (Tropomi), due to the more difficult mounting and the 'aggressive' shape with large slopes. This required a very low turning speed, which in turn required very high thermal stability of the cutting tool (<10 nm over a period of minutes or more). Also the effective aperture was only ~1 mm smaller than the edge of the mirrors. The grating was a COTS item procured from Jobin Yvon.



**Fig. 3.** The four Spectrolite mirrors after manufacturing

The mirrors and the grating were assembled on manufacturing tolerance, which took approximately 1.5 days. The detector was mounted and aligned on shims. The detector alignment was an iterative process between measurements with different shims and optical model predictions. Finally, the detector was positioned on using 'ideal' shims. The whole alignment of the detector was done in approximately one day.

### C. Spectrolite Breadboard performance

In order to verify the performance of the Spectrolite Breadboard a number of test and analyses have been performed, focusing on the following main performance parameters:

- The (RMS) spatial spot size
- The (RMS) spectral spot size
- The spectral range
- Co-registration
- Signal to Noise (S/N)

A more detailed description of these verification activities falls outside of the scope of this paper and can be found in Ref [2]. Here we only present the achieved results.

The spectral range has been determined by illuminating the BB using several spectral line source coupled into a small integrating sphere (see Fig. 4 for the HgAr measurement result). Using these measurements the grating function was fitted and the spectral range calculated to be 300 nm to 490 nm. Using the same measurements also the spectral resolution was determined and found to be below 0.35nm (see Fig. 5).

The spatial and spectral spot sizes were measured using mono-chromatic star stimuli and were found to be  $\sim 20 \mu\text{m}$ , well within the required spot sizes. This measurement confirmed that the instrument should be able to achieve the required spatial resolution.

The co-registration or spatial straightness was measured using the same star stimulus, but now with a white light sources. In this way an entire spectrum of a single spatial position was imaged on the detector. Based on the analysis performed, the spectral straightness was found to be better than  $10 \mu\text{m}$  over the entire spectral range.

Finally the expected signal to noise of the demonstrator was calculated for an in-orbit spectral radiance corresponding to an albedo of  $\sim 5\%$  in the spectral range of 400 nm - 500 nm. Due to the limited etendue (less light efficient), limited transmission (more light loss), lower spectral resolution (less photons per pixel) and the use of a commercial detector (more noise) in the BB the SNR is  $\sim 70$ .

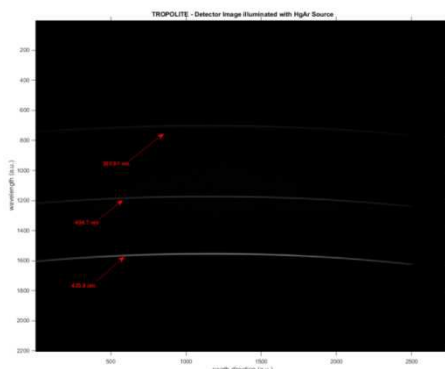


**Fig. 4.** Spectral calibration. Detector frame; the three lines correspond to 365, 405 and 436 nm

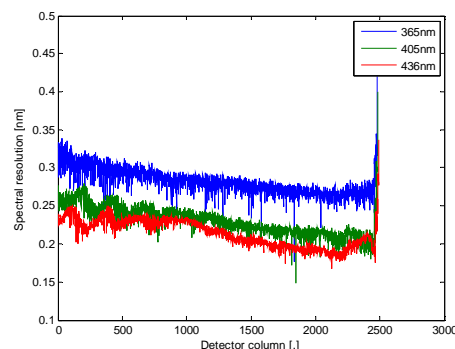


**Fig. 5.** Spectral resolution over the entire slit.

### III FROM LABORATORY BREADBOARD TO AIRBORNE INSTRUMENT

At the end February 2016 TNO was presented with the opportunity to participate in an airborne measurement campaign called AROMAPEX [7], which was coordinated by BIRA. The flight was considered to be a good opportunity to test the Spectrolite concept in realistic circumstances. In accepting the opportunity TNO also took on the challenge to transform the cleanroom environment breadboard model (Fig. 6) into a fully autonomous, temperature controlled, calibrated flight instrument. For this a number of challenges had to be solved:

*A. Temperature*

The test flight would be executed at an altitude of 3 km. At this altitude the outside temperature is several °C below zero, while the breadboard was only tested and verified in stable cleanroom conditions. The expected low temperatures were seen as a problem because it potentially leads to water condensation inside the instrument. In addition it may lead to a different instrument performance when compared to previous breadboard characterization in the laboratory. In order to overcome these challenges, an external housing (see Fig. 7) was designed to encapsulate the Spectrolite BB and shield it against external influences. Furthermore, a thermal control system was added consisting of terrarium heater pads and a basic thermal control system (see <http://www.komodoproducts.com/products/heating> for more details). This allowed the instrument to operate at a temperature of 25°C with a stability of +/-0.5°C during the entire flight. Fig. 8 shows the temperatures at different locations on the instrument during one of the flights. This relatively stable temperature ensured nominal performance and prevented water condensation inside of the instrument.

*B. Contamination*

Because the flight instrument was to be mounted on the bottom plate of a Cessna T207A with an open viewing hole to ground, there were concerns about contamination from outside air and aircraft exhaust products on the optical components. Therefore an additional glass transmission window was added to fully close the housing. By installing a heater pad close to the window, the problem of water condensation was solved as well.

*C. Mechanical vibrations*

The motor of a Cessna T207A introduces vibrations into the fuselage of the aircraft. Because the instrument is directly bolted to the aircraft fuselage, it is exposed to these vibrations, which could hamper the performance of the overall instrument. Seen the instantaneous field-of-view of only 0.051°arc, the smallest angular rotation would disturb the instrument performance. Therefore, in order to isolate Spectrolite from these vibrations, rubber isolators were introduced as a precaution. However, no measurements were performed to characterize the remaining vibrations in the instrument.

*D. Calibration and characterization*

Space optical spectrometer instruments are normally characterized for several months during an on-ground calibration campaign. Such a period was not available for the Spectrolite instrument prior to the flight and thus a compact characterization approach was set-up, taking only for a few days of measurement time. More details about this approach can be found in the next chapter (IV).

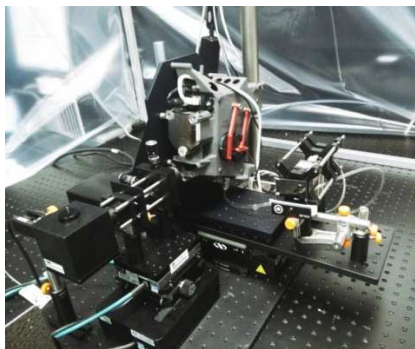


**Fig. 6.** Spectrolite BB in TNO cleanroom

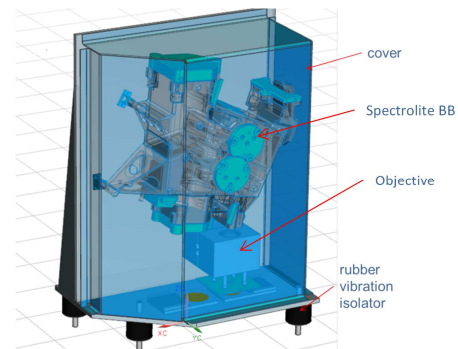


**Fig. 7.** Spectrolite flight instrument

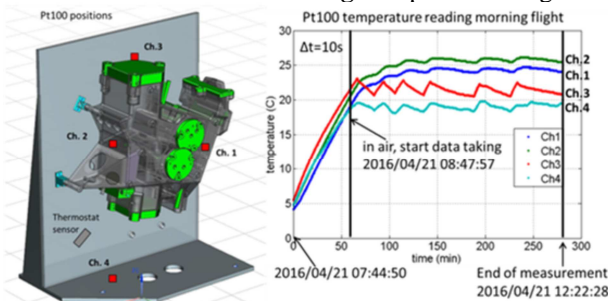


**Fig. 8.** Spectrolite achieved Temperature profile during flight.  
Proc. of SPIE Vol. 10562 105621N-6

#### IV LEVEL 0-1B DATA PROCESSOR AND CHARACTERISATION

For the Berlin Spectrolite test flight a dedicated data processor (Fig. 9) was designed. The function of this data processor was to convert the raw detector images in to spectral radiance data of the atmosphere that can be used in NO<sub>2</sub> concentration retrieval. In the design of the data processor also the time constraint of “a few days” for performing the characterization was taken into account. The data processor consisted of a number of correction steps and corresponding key data products (characterization data necessary to perform a certain calibration step). The following correction steps were introduced:

##### *A Bad pixel removal*

During this step all pixels identified as being a “dead” or “bad” pixel are removed from the data. This removal is performed on the basis of a “bad pixel map”, which was determined based on ground dark and illuminated measurement. The removed pixels were replaced with an interpolated data point.

##### *B Electronics offset and dark current removal*

During this step the electronics offset and dark current signal are subtracted on a pixel to pixel basis. The electronics offset and dark current are subtracted in different steps because the electronics offset is constant with integration time, while the dark current varies linearly (first order) with the dark current. The subtraction is performed on the basis of electronics offset and dark current key data that has been determined during an on ground dark measurement with several integration times.

##### *C Flat fielding and radiometric calibration*

During this step the pixel data is transformed from [BU] to spectral radiance levels per pixel. This setup includes all radiometric effects being pixel to pixel response variations, slit width variations (physical dimension changes of the slit over the swath), spectral quantum efficiency variations and conversion to radiance levels are taken care of. In most space instruments these steps are performed separately, but for convenience and time reduction these steps were combined in this case.

For this correction a pixel based radiometric response map was generated and applied to the data. The radiometric response map has been generated on the basis of a measurement with an integrating sphere, which spectral radiance was made absolute through the calibration of the GOME 2 instrument. This means that the radiometric calibration can be traced back to a NIST standard calibrated light source, assuming that the sphere has not degraded over time the accuracy should be in the order of 2% to 5%.

##### *D Wavelength map*

Finally the data was augmented with a pixel based wavelength map, identifying the central wavelength measured by each pixel. This map was based on measurements with a spectral line source.

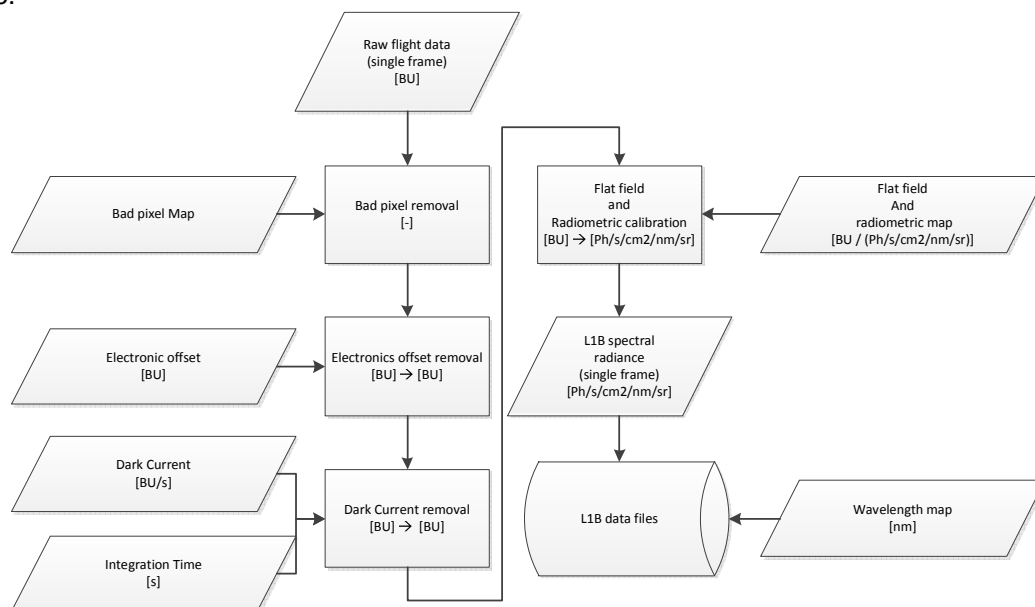


**Fig. 9.** Spectrolite Berlin flight L0-1B data processor.

## V BERLIN FLIGHT NO2 RETRIEVAL RESULTS

The AROMAPEX [7] campaign provided an excellent opportunity to test the Spectrolite instrument under atmospheric conditions and to compare NO<sub>2</sub> retrievals with those obtained with other similar instruments such as APEX [4], AirMAP [5] and SWING [6]. Much of this work remains to be done and will be described in future publications. In this paper we describe the procedure that was applied to derive differential slant NO<sub>2</sub> columns from the Spectrolite spectra and discuss the results by comparing the spatial patterns observed during the flight of 21 April 2016 with those obtained by the other groups.

Tropospheric NO<sub>2</sub> columns measured from an aircraft flying at 3km altitude contain mostly information about the vertically integrated amount of NO<sub>2</sub> in the boundary layer, hence they provide an estimate of boundary layer pollution. Retrieval of tropospheric NO<sub>2</sub> vertical columns (VCD) from Spectrolite L1B spectra consists essentially of two steps. The first is to derive differential slant NO<sub>2</sub> columns (DSCD) by application of the spectral analysis procedure called DOAS (differential optical absorption spectroscopy, see also Ref [8]). The second step is the conversion of DSCD to VCD's by application of the air mass factor (AMF), which accounts for all factors affecting the DSCD, but which are not related to the VCD: the solar zenith angle, instrument viewing zenith angle, relative azimuth angle, NO<sub>2</sub> and aerosol vertical distribution (profile shapes), aerosol optical thickness and surface reflectance. Loosely speaking, the DSCD can be understood as the number of NO<sub>2</sub> molecules/cm<sup>2</sup> encountered along the average photon path from the sun through the atmosphere to the detector, relative to the same quantity corresponding to the reference spectrum (see below).

In this paper we describe in more detail the first step (DSCD retrieval). We focus on this intermediate product partly because implementation of step two is currently (August 2016) still ongoing, but also because the DSCD product already provides valuable insights in the abilities of the Spectrolite instrument. Challenges with regard to the VCD retrieval in step two are largely related to AMF simulations and therefore on the availability of suitable a-priori information.

Ground pixels of Spectrolite with the telescope used in this study are approximately 5m (across track) by 11m (along track). These pixels are however too small for NO<sub>2</sub> retrievals so before the actual DOAS analysis is performed spectra are added in order to obtain a sufficient signal to noise ratio. For practical reasons pixels are added in the direction of flight, resulting in rather elongated pixels (approximately 5m in across track direction and 264m in along track direction) because of the narrow pixel width in across track direction (74 viewing directions). It should be noted that different procedures shall be explored in the near future in order to obtain pixels with aspect ratios close to one and a similar signal to noise ratio for NO<sub>2</sub>, for instance pixels of 35x33m.

After adding the spectra, spectral calibration is refined by comparing the measured spectrum to a solar spectral atlas (Kurucz). This is achieved by simultaneously fitting a third order polynomial describing the pixel to wavelength mapping of the radiance spectrum and (the width of) a Gaussian representing the slit function that is applied to the Kurucz spectrum (see Fig. 10b). The resulting slit function is then applied to the trace gas cross sections before differential absorption cross sections are obtained.

The DOAS procedure itself can be seen as a curve fitting technique where differential absorption cross sections of relevant trace gases  $\Delta\sigma_i(\lambda)$  are fitted to the differential optical thickness spectrum that can be derived from the radiance spectrum measured by Spectrolite. This is described by the following equation:

$$\ln\left(\frac{I_{ref}(\lambda)}{I(\lambda)}\right) - P(\lambda) = \sum_i \Delta\sigma_i(\lambda) \cdot N_i^s, \quad (1)$$

and the result is illustrated in Fig. 10. The differential optical thickness spectrum is described on the left hand side of the equation. Here  $P(\lambda)$  is a low order polynomial (we used order 5),  $I(\lambda)$  is the radiance spectrum to be analyzed and  $I_{ref}(\lambda)$  is the reference spectrum (see below). The DSCDs (denoted  $N_i^s$ ) are the outcome of the fitting procedure, i.e. the scaling factors corresponding to the differential cross sections of every trace gas  $i$ . Also the differential Ring spectrum is included in the fit, in order to account for the Ring effect caused by inelastic scattering of photons in the atmosphere. The Ring spectrum is treated as a pseudo-absorber, and for that reason not separately mentioned in the above equation.

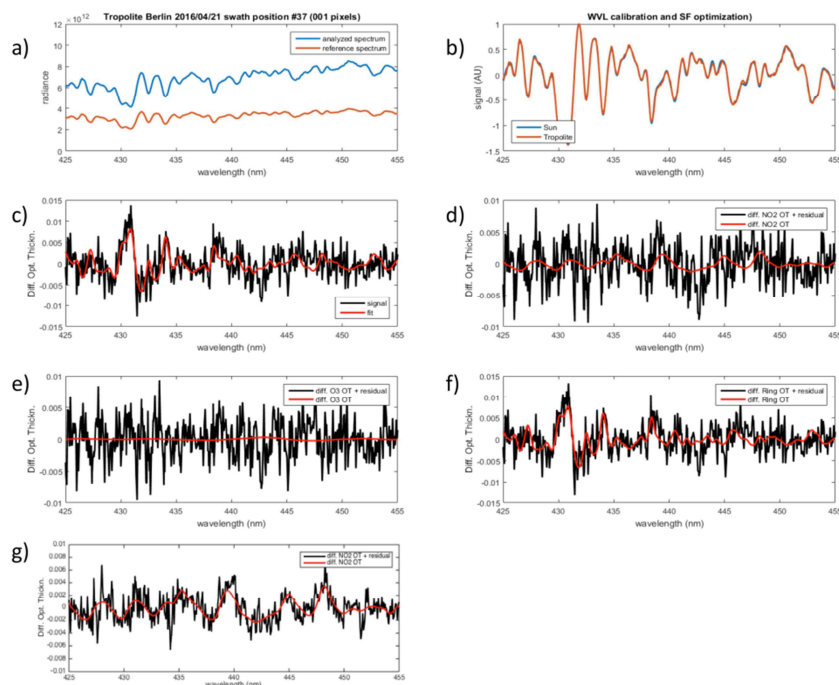


**Fig. 10.** An example of DOAS analysis of two spectra (one of which is reference spectrum). a) radiance spectra; b) differential structures of measured spectrum are aligned with differential structures in solar spectrum in wavelength calibration procedure ; c) differential optical thickness spectrum compared to fit result (i.e. the sum of the red curves shown in panels d), e) and f) ; d) fit result for NO<sub>2</sub> ; e) fit result for ozone ; f) fit result for Ring cross section ; g) NO<sub>2</sub> fit result for different spectrum, namely one obtained after adding 125 spectra instead of 24 (figures a-f).

Fig. 10 shows that it is essential to include the Ring spectrum in the DOAS fit, as it comprises the largest contribution to the fitted curve (10c). This can probably be related to the considerable difference in radiance levels between the spectrum to be analyzed and the reference spectrum (10a): a different radiance level indicates a different surface reflectance hence a different distribution of photon paths. Ozone does not have a relevant contribution to the DOAS fit which is partly due to the relative weak differential ozone absorption structures in this wavelength range, and partly due to the fact that apparently the tropospheric ozone levels do not vary that much between the two spectra.

It is quite remarkable to see on the one hand the relatively large mean amplitude of the residual compared to the NO<sub>2</sub> signal (indicating an imprecise fit) and on the other hand the consistency of NO<sub>2</sub> retrievals between adjacent pixels, as discussed below (Fig. 12). Fig. 10g shows that averaging five times more spectra considerably improves the NO<sub>2</sub> fit but it will not reveal significantly more spatial detail as this effectively reduces the spatial resolution. A different way to improve the signal to noise ratio of the NO<sub>2</sub> fit is to add more spectra to the reference spectrum. This can be done if the instrument is sufficiently stable (spectrally).

One should be aware that DSCDs are defined relative to the reference spectrum  $I_{ref}(\lambda)$ . Whereas in case of satellite measurements a direct (irradiance) measurement of the Sun can be used as reference, this is not possible for airborne observations. As a consequence, we use as reference a radiance spectrum that is measured during the flight and we obtain DSCDs relative to this reference. Although in principle any spectrum can be selected as reference, it is common practice to select a spectrum measured over a region with relatively low pollution levels, such that high pollution levels at other locations correspond to positive DSCDs. An additional advantage of this approach to select a reference spectrum is that the need for a stratospheric NO<sub>2</sub> correction is strongly reduced, especially when observations are done in a period with relatively little variability in the solar zenith angle, hence a quite constant average photon path length through the stratosphere. In the case of 21 April, a region on the West side of the domain was used as reference region (see fig. 11).

Fig. 11 shows the map providing an overview of differential slant NO<sub>2</sub> columns (DSCD) measured in the morning and afternoon of 21 april 2016 over the city of Berlin and surrounding regions. The most

striking feature of both maps is the pollution plume over the city center, stretching out from West to East. This feature was also observed with the other instruments (APEX, AirMAP and SWING) participating in the AROMAPEX campaign and gives a first indication of successful operation of Spectrolite.



Fig. 11. Map of  $\text{NO}_2$  DSCD's retrieved during afternoon flight over Berlin on 21 April 2016.

Apart from this main feature, it can be seen when looking in more detail that quite often adjacent pixels show considerably different  $\text{NO}_2$  DSCDs. This is in general not expected to be due to true variability in the tropospheric  $\text{NO}_2$  column field. Especially over urban regions away from strong local  $\text{NO}_x$  sources it can be expected that the true  $\text{NO}_2$  column between adjacent pixels differs only by a few percent. For the largest part the differences between adjacent pixels are due to relatively low signal to noise, i.e. imprecise DOAS fits, but also differences in surface reflectance between adjacent pixels partly explain the differences in  $\text{NO}_2$  DSCD. Bright surfaces (often white painted buildings or concrete infrastructure) cause enhanced sensitivity to  $\text{NO}_2$  close to the surface. On the opposite, over dark surfaces (e.g. forests) the same  $\text{NO}_2$  VCD will go along with a lower DSCD because of reduced sensitivity.

Fig. 12 provides a more detailed view on typical differences between adjacent pixels, and how these compare to the main features that can be seen on the map (e.g. the pollution plume over the city center). Adjacent pixels, either in along-track or in across-track direction, show differences in  $\text{NO}_2$  DSCD of roughly  $3\text{-}5 \times 10^{15} \text{ molec/cm}^2$ . This is sufficient to detect the plume, i.e. to quantify the contrast between pollution in the city center and rural regions at greater distance from the center. Fig. 11 and 12 clearly show the broadening of the plume downwind of the main sources (power plants in the Western part of the city) and the scattered sources within the city itself (e.g. traffic). Not only the plume broadens, but also the background appears to be more and more affected by sources upwind. One should however be careful to interpret this upward trend of background levels in terms of changes in  $\text{NO}_2$  VCD alone. As the total duration of the flight is more than one hour, the solar position may change considerably with respect to the solar position at the time of reference. This may cause an effect on  $\text{NO}_2$  DSCDs that should carefully be considered when deriving the differential AMFs before converting to VCDs.

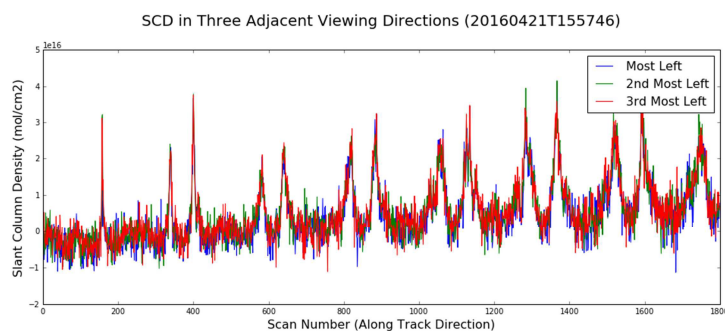


Fig. 12.  $\text{NO}_2$  DSCD as a function of scan number in along track direction for the leftmost three out of a total of 74 viewing directions (directly adjacent). Major peaks correspond the region of the pollution plume over the city, as can be seen in Fig. XY.

## VI CONCLUSIONS AND NEXT STEPS

### A. Conclusion

The Spectrolite instrument concept has been successfully developed and converted in a breadboard that has been flown on the AROMAPEX aircraft campaign.

The Spectrolite data generated during the AROMAPEX aircraft has been (partially) analyzed and shows a good comparison with the other instruments that were part of the same aircraft campaign.

### B. Next Steps

Spectrolite will be further developed as part of a consortium of several industrial and institutional partners. The consortium consist of Airbus DS Netherlands, ISIS, S&T and TNO. The consortium will be supported by KNMI for data retrieval support. The consortium aims at achieving a Spectrolite CDR/MRR level within 1 year and aims for a system with a ground sampling distance of 1x1km and a Signal to Noise > 500 (for urban areas).

In parallel the NO<sub>2</sub> retrieval of the Berlin flight will be refined. The results of these studies will be invaluable and supporting for the further development of Spectrolite.

### C. Acknowledgements

The authors of this paper would like to acknowledge all the partners of the AROMAPEX campaign for allowing Spectrolite to join the measurement campaign above Berlin and for their support during the data interpretation.

Special thanks also go to the aircraft operators of the Free University of Berlin for their patience and support during the Spectrolite flight preparations. Without their support a conversion into a flying Spectrolite would not have been possible.

## REFERENCES

- [1] L. Maresi, W. van der Meulen, R. Vink. “*TROPOLITE, on the path of Atmospheric Chemistry Made Simple*”, Proc. SPIE 9241, 92410J, 2014
- [2] L.F. van der Wal, B.T.G. de Goeij, R. Jansen, et. al., “*COMPACT, LOW-COST EARTH OBSERVATION INSTRUMENTS FOR NANO- AND MICROSATELLITES*”, Small Satellites Systems and Services Symposium, May-June 2016.
- [3] Volatier J-P., Bäumer S., Kruizinga B. and Vink R., “*Case study: TROPOLITE*”, Proc. SPIE 9131, 91310L, May 1, 2014.
- [4] Popp, C., Brunner, D., Damm, A., Van Roozendael, M., Fayt, C., and Buchmann, B.: High-resolution NO<sub>2</sub> remote sensing from the Airborne Prism EXperiment (APEX) imaging spectrometer, Atmos. Meas. Tech., 5, 2211-2225, doi:10.5194/amt-5-2211-2012, 2012.
- [5] Schönhardt, A., Altube, P., Gerilowski, K., Krautwurst, S., Hartmann, J., Meier, A. C., Richter, A., and Burrows, J. P.: A wide field-of-view imaging DOAS instrument for two-dimensional trace gas mapping from aircraft, Atmos. Meas. Tech., 8, 5113-5131, doi:10.5194/amt-8-5113-2015, 2015.
- [6] Merlaud, A., Constantin, D., Mingireanu, F., Mocanu, I., Fayt, C., Maes, J. Murariu, G., Voiculescu, M., Georgescu, L., Van Roozendael, M.: Small whiskbroom imager for atmospheric composition monitoring (SWING) from an unmanned aerial vehicle (UAV), [Proc. 21st ESA symposium on european rocket and balloon programmes and related research, Thun, Switzerland, June 2013](#)
- [7] <http://www.eufar.net/weblog/2016/06/15/inter-comparison-airborne-atmospheric-imagers-during-aromapex-campaign/>
- [8] Platt, U. and Stutz, J., Differential Optical Absorption Spectroscopy: Principles and Applications, Springer, 2008.